UCLA

UCLA Previously Published Works

Title

Tempering stochastic density functional theory

Permalink

https://escholarship.org/uc/item/9fs0973k

Journal

The Journal of Chemical Physics, 155(20)

ISSN

0021-9606

Authors

Nguyen, Minh

Li, Wenfei

Li, Yangtao

et al.

Publication Date

2021-11-28

DOI

10.1063/5.0063266

Copyright Information

This work is made available under the terms of a Creative Commons Attribution-NonCommercial License, available at https://creativecommons.org/licenses/by-nc/4.0/

Peer reviewed

eScholarship.org Powered by the California Digital Library
University of California

arXiv:2107.06218v2 [physics.comp-ph] 16 Oct 2021

Tempering stochastic density functional theory

Minh Nguyen, Wenfei Li, Yangtao Li
Department of Chemistry and Biochemistry, University of California at Los Angeles, Los Angeles, California 90095, USA

Eran Rabani
Department of Chemistry, University of California and Materials Sciences Division, Lawrence Berkeley National Laboratory, Berkeley, California 94720, USA and The Raymond and Beverly Sackler Center of Computational Molecular and Materials Science, Tel Aviv University, Tel Aviv 69978, Israel

Roi Baer
Fritz Haber Center of Molecular Dynamics and Institute of Chemistry, The Hebrew University of Jerusalem, Jerusalem, 91904 Israel

Daniel Neuhauser*
Department of Chemistry and Biochemistry, University of California at Los Angeles, and California Nanoscience Institute, Los Angeles, California 90095, USA

We introduce a tempering approach with stochastic density functional theory (sDFT), labeled t-sDFT, which reduces the statistical errors in the estimates of observable expectation values. This is achieved by rewriting the electronic density as a sum of a "warm" component complemented by "colder" correction(s). Since the warm component is larger in magnitude but faster to evaluate, we use many more stochastic orbitals for its evaluation than for the smaller-sized colder correction(s). This results in a significant reduction in the statistical fluctuations and systematic deviation compared to sDFT for the same computational effort. We demonstrate the method's performance on large hydrogen-passivated silicon nanocrystals, finding a reduction in the systematic deviation in the energy by more than an order of magnitude, while the systematic deviation in the forces is also quenched. Similarly, the statistical fluctuations are reduced by factors of ≈4-5 for the total energy and ≈1.5-2 for the forces on the atoms. Since the embedding in t-sDFT is fully stochastic, it is possible to combine t-sDFT with other variants of sDFT such as energy-window sDFT and embedded-fragmented sDFT.

I. INTRODUCTION

Kohn-Sham density functional theory (KS-DFT) is widely used for calculating the properties of molecular and extended systems [1]. In particular, the method is useful for determining the structure based on the estimates it provides for the forces on the corresponding nuclei [2–4]. However, applying KS-DFT for systems with hundreds or thousands of atoms is challenging due to the high scaling of computational costs with a system's size (potentially quadratic but eventually cubic for large systems). Lower scaling implementations of the theory have been developed for systems that have a density matrix that is fairly sparse so that only a linear-scaling near-diagonal portion of the matrix needs to be processed. Because of the restriction to near-localized density matrices, the use of such methods is often limited to low-dimensional structures [5, 6] or systems with strictly localized electrons [7, 8].

In previous work we introduced stochastic density functional theory (sDFT) [9] which avoids the costly diagonalization step in KS-DFT without the need to make a locality assumption; instead, the density matrix is approximated statistically. Specifically, the density matrix in sDFT is viewed as a correlation function of stochastic functions, each of which is, in essence, a random combination of the occupied states. While the method scales linearly, the tradeoff is the introduction of statistical uncertainties in the density and other observables. The statistical errors can be reduced by using an embedded-fragmented (ef-sDFT) technique [10–12] which is based on dividing the system into fixed-size fragments and expressing the total electron density, $n(\boldsymbol{r})$, as the sum of fragment densities plus a correction term which is evaluated stochastically. This technique reduces the statistical fluctuations in the estimates of the atomic forces and the energies [10, 11], and the magnitude of this reduction is controlled by varying the size of the fragments and the number of stochastic realizations. An additional approach for mitigating the statistical errors is the energy-window sDFT (ew-sDFT)

* Corresponding Author: Daniel Neuhauser, dxn@ucla.edu

scheme [13] and its combination with the embedded-fragmented technique [10, 14].

Here we propose a tempering method, referred to as t-sDFT, as a complementary technique for reducing the statistical noise. In t-sDFT, the density for the desired temperature is calculated using a higher-temperature reference density with smaller correction(s). This idea has been implemented before within the energy renormalization group in the context of telescopically expanding the Hamiltonian matrix in a series [15]. In Sec. II, we describe the t-sDFT method and in Sec. III we benchmark and analyze its efficacy using large hydrogenated silicon clusters. Sec. IV we discuss the conclusions and summarize.

II. METHODOLOGY

A. Stochastic Density Functional Theory

Our starting point is the following expression for the electron density, $n(\boldsymbol{r})$ (assuming a spin-unpolarized system) [9]:

$$n(\boldsymbol{r}) = 2 \times \mathrm{Tr}\left[\sqrt{\hat{\rho}_\beta}\,|\boldsymbol{r}\rangle\langle\boldsymbol{r}|\,\sqrt{\hat{\rho}_\beta}\right], \tag{1}$$

where $\boldsymbol{r}$ is a point on a 3D grid that spans the space containing the electron density of the system and has a volume element dV. The operator

$$\hat{\rho}_\beta = f_{\beta\,\mu}\left(\hat{h}\right) \tag{2}$$

is a low band-pass Fermi-Dirac (FD) filter. Our main interest in this paper is zero-temperature DFT; however, to efficiently represent the density matrix, a smooth step function must be used, and the simplest is a Fermi-Dirac distribution, $f_{\beta\,\mu}(\varepsilon) = \left(1+e^{\beta(\varepsilon-\mu)}\right)^{-1}$, which blocks high energies ($\varepsilon > \mu+\beta$). Here, the chemical potential, μ, must be adjusted such that the integrated density equals the number of electrons, N_e,

$$\int n(r)dV = \sum_{\boldsymbol{r}} n(\boldsymbol{r})\,dV = N_e, \tag{3}$$

while β is the inverse temperature (note that the filter, $\hat{\rho}_\beta$, depends on the chemical potential but to avoid a plethora of indices we do not explicitly note this dependence below). In the low-temperature limit ($\beta\varepsilon_{\mathrm{gap}} \gg 1$, where $\varepsilon_{\mathrm{gap}}$ is the fundamental KS gap), $n(\boldsymbol{r})$ indeed converges to the ground state KS-density. Further, as our goal here is not finite-temperature DFT, we use the usual zero-temperature DFT exchange-correlation functionals.

In Eq. (2), the Kohn-Sham Hamiltonian is:

$$\hat{h} = \hat{t} + \hat{v}[n](\boldsymbol{r}) \tag{4}$$

where $\hat{t}$ is the kinetic energy operator and $\hat{v}[n](\boldsymbol{r})$ is the density-dependent KS potential that is composed of electron-nuclei, Hartree, and exchange-correlation components. Eqs. (1)-(4) must be solved simultaneously to yield the self-consistent electron density.

In sDFT, we introduce a stochastic resolution of the identity [16] which transforms the trace in Eq. (1) to an expectation value [9]

$$n(\boldsymbol{r}) = 2\left\langle \left| \left\langle \boldsymbol{r} \left| \sqrt{\hat{\rho}_\beta} \right| \chi \right\rangle \right|^2 \right\rangle_\chi, \tag{5}$$

where $|\chi\rangle$ is a stochastic orbital taking the randomly signed values $\langle\boldsymbol{r}\,|\chi\rangle = \pm(dV)^{-1/2}$.

To apply the filter, $\sqrt{\hat{\rho}_\beta}$, we use a Chebyshev expansion of length K [17]

$$\sqrt{\hat{\rho}_\beta}\,|\chi\rangle = \sum_{k=0}^{K} c_k(\beta,\mu)\left|\zeta^{(k)}\right\rangle, \tag{6}$$

where $\left|\zeta^{(k)}\right\rangle = T_k(\hat{h}_s)\,|\chi\rangle$ are defined by the Chebyshev polynomial recursion relations: $\left|\zeta^{(0)}\right\rangle = |\chi\rangle$, $\left|\zeta^{(1)}\right\rangle = |\chi\rangle$ and $\left|\zeta^{(k+1)}\right\rangle = 2\hat{h}_s\left|\zeta^{(k)}\right\rangle - \left|\zeta^{(k-1)}\right\rangle$. Here, $\hat{h}_s = \left(\hat{h}-\bar{\varepsilon}\right)/\Delta\varepsilon$ is a normalized KS Hamiltonian where $\bar{\varepsilon}$ and $\Delta\varepsilon$ are chosen such that the spectrum of $\hat{h}_s$ lies within the interval $[-1,1]$, $T_k(x)$ is the k'th Chebyshev polynomial, and $c_k(\beta,\mu)$ are the Chebyshev expansion coefficients of the filter $\sqrt{f_\beta(\varepsilon)}$[17]. The expansion length K terminates the series when $|c_{k>K}|$ is smaller than a predetermined cutoff value.

In practice, the expected value appearing in Eq. (5) is evaluated approximately by taking a finite sample of N_s stochastic orbitals:

$$n(\boldsymbol{r}) \approx \frac{2}{N_s}\sum_{i=1}^{N_s}\left|\left\langle \boldsymbol{r}\left|\sqrt{\hat{\rho}_\beta}\right|\chi_i\right\rangle\right|^2. \tag{7}$$

Furthermore, to ensure $N_e = \sum_{\boldsymbol{r}} n(\boldsymbol{r})\,dV$, we tune the chemical potential μ to satisfy the relation:

$$N_e = 2\sum_{k=0}^{K} b_k(\beta,\mu)\,M_k, \tag{8}$$

where

$$M_k = \frac{1}{N_s}\sum_{i=1}^{N_s}\left\langle \chi_i \left| \zeta_i^{(k)} \right\rangle \right. \tag{9}$$

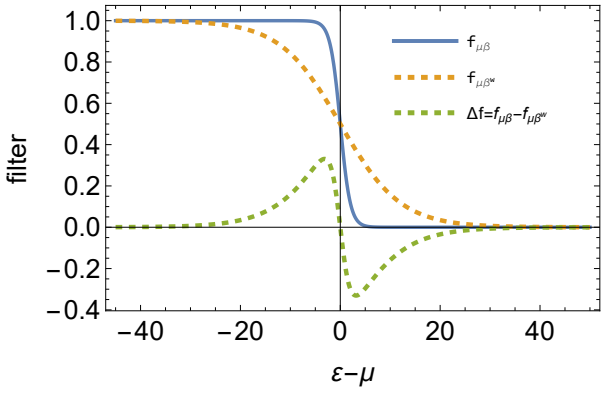

Figure 1. The desired low-temperature filter, $f_{\beta\,\mu}(\varepsilon)$, the high-temperature filter $f_{\beta^w\,\mu}(\varepsilon)$, and the correction for $\beta = 6\beta^w$.

are the stochastic estimates of the Chebyshev moments [18] and $b_k(\beta,\mu)$ are the Chebyshev expansion coefficients of the function $f_{\beta\,\mu}(\varepsilon)$ as opposed to $c_k(\beta,\mu)$ which are the expansion coefficients of $\sqrt{f_{\beta\,\mu}(\varepsilon)}$.

As a result of using stochastic orbitals, the sDFT density and associated observables have two additional types of errors. One is the usual stochastic fluctuations that scale as $\mathrm{O}(N_s^{-\frac{1}{2}})$, but in addition, there is a systematic deviation which scales as $\mathrm{O}(N_s^{-1})$ that appears due to the nonlinear SCF procedure (the filtering operator applied on each orbital depends on the density, which itself depends on the set of filtered orbitals).

Increasing the number of sampling orbitals, N_s, will decrease both types of errors, at the cost of additional work.

To measure the computational cost of a sDFT or t-sDFT calculation, we use a numerical "work" quantity, W, which is the total number of Hamiltonian operations performed per SCF cycle (i.e., action by the Hamiltonian on a function), which for sDFT is approximately

$$W \simeq KN_s.$$

In practice, the work needs to be multiplied by a factor of about 1.7 due to the need to determine μ based on Eq. (8), but since this factor is common to all our methods here we do not include it.

B. Tempering Stochastic Density Functional Theory

We now describe the tempering method, designed to reduce the statistical errors in sDFT without increasing the overall computational effort. Consider, the decomposition of the desired filter, $\hat{\rho}_\beta$ (see Eq. (2)), into a higher temperature filter, $\hat{\rho}_{\beta^w}$ ($\beta^w < \beta$), with the correction term:

$$\Delta\hat{\rho} = \hat{\rho}_\beta - \hat{\rho}_{\beta^w}, \tag{10}$$

which is shown in Fig. (1) for a typical case of $\beta/\beta^w = 6$. Note that (a) all values of $\Delta\hat{\rho}$ are much smaller than unity and (b) the high-temperature filter, $\hat{\rho}_{\beta^w}$, is smoother than the low-temperature one, so its Chebyshev expansion is shorter (the Chebyshev expansion length of $\hat{\rho}_\beta$ is proportional to β [9]).

The electron density in Eq. (5) can therefore be written as $n(\boldsymbol{r}) = n_{\beta^w}(\boldsymbol{r}) + \Delta n(\boldsymbol{r})$, where the two terms are evaluated separately using two distinct independent sets of stochastic orbitals: χ_i^w, $i = 1,\ldots,N_s^w$ for the warmer density,

$$n_{\beta^w}(\boldsymbol{r}) = \frac{2}{N_s^w}\sum_{i=1}^{N_s^w}\left|\left\langle \boldsymbol{r}\left|\sqrt{\hat{\rho}_{\beta^w}}\right|\chi_i^w\right\rangle\right|^2 \tag{11}$$

and χ_i^Δ, $i = 1,\ldots,N_s^\Delta$ for the correction term,

$$\Delta n(\boldsymbol{r}) = \frac{2}{N_s^\Delta}\sum_{i=1}^{N_s^\Delta}\left(\left|\left\langle \boldsymbol{r}\left|\sqrt{\hat{\rho}_{\beta}}\right|\chi_i^\Delta\right\rangle\right|^2 - \left|\left\langle \boldsymbol{r}\left|\sqrt{\hat{\rho}_{\beta^w}}\right|\chi_i^\Delta\right\rangle\right|^2\right). \tag{12}$$

As demonstrated in Fig. 1, the correction density, $\Delta n(\boldsymbol{r})$, is much smaller than the warm density, $n_{\beta^w}(\boldsymbol{r})$, which is similar in overall magnitude to the total density. This gives the key for the efficiency of the tempering approach as compared to the original sDFT calculation. Specifically, compared to an sDFT calculation with polynomial expansion length K and N_s stochastic orbitals and aiming for the same overall work as in sDFT, we get that:

- The computational work required to calculate the warm density is $W^w \simeq K^w N_s^w$. Since the Chebyshev expansion lengths are proportional to β, the warmer temperature density $n_{\beta^w}(\boldsymbol{r})$ requires a much *shorter* Chebyshev expansion length than the original sDFT density ($K^w = \frac{\beta^w}{\beta}K$), so many more stochastic orbitals can be used to evaluate it for the same overall computational cost (i.e., $N_s^\Delta \gg N_s$).

- The computational work for correction term, $\Delta n(\boldsymbol{r})$, is $W^\Delta \simeq KN_s^\Delta$ as both terms in the RHS of Eq. (12) use the same set of $\left|\zeta_i^{\Delta,(k)}\right\rangle = T_k(\hat{h}_s)\left|\chi_i^\Delta\right\rangle$ (the two terms differ in their expansion coefficients). Since the numerical magnitude of the correction term is much smaller than that of the overall density, its standard deviation is correspondingly much smaller. Therefore the numerical effort (i.e.,

System	Band-gap	β	Correction filter			Warm filter			W^{tot}
	(eV)	(eV^{-1})	K	N_s^Δ	$W^\Delta = KN_s^\Delta$	K^w	N_s^w	$W^w = K^w N_s^w$	
$Si_{35}H_{36}$	3.4	1.83	2000	6	12,000	$K \times \beta^w/\beta$	$24 \times \beta/\beta^w$	48,000	60,000
$Si_{87}H_{76}$	2.5	2.94	3200	6	19,200	$K \times \beta^w/\beta$	$24 \times \beta/\beta^w$	76,800	96,000
$Si_{353}H_{196}$	1.6	4.60	5000	6	30,000	$K \times \beta^w/\beta$	$24 \times \beta/\beta^w$	120,000	150,000

Table I. The Chebyshev expansion lengths, K and K^w, and the number of stochastic orbitals, N_s^Δ and N_s^w, used in our simulations. We also show the required numerical work, W, defined as the number of Hamiltonian operations. Note that for each system we increase the number of high-temperature orbitals (N_s^w) with temperature (i.e., with increasing β/β^w) such that the total work W^{tot} is independent of β/β^w.

the number of samples required for a given accuracy), which is proportional to the squared standard deviation, is much smaller for the correction term, so it is sufficient to use fewer stochastic orbitals ($N_s^\Delta \ll N_s$) to achieve a similar statistical error.

Here, K^w and K are respectively the Chebyshev expansion lengths for the warm reference density and the correction term, with $\frac{K^w}{K} = \frac{\beta^w}{\beta} \ll 1$ (note that since the correction term involves the original low-temperature density, the number of Chebyshev terms it requires, K, is the same as in the original sDFT). Overall, the partitioning of the filter into a larger component at a higher temperature with a shorter Chebyshev expansion, and a smaller correction term, offers an additional knob to control the statistical error by using $N_s^w \gg N_s$ without increasing the overall computational effort.

The use of tempering modifies how the chemical potential is calculated. Instead of fulfilling the single-sum sDFT constraint on the residues (Eq. (8)), the chemical potential is adjusted to satisfy the following relation which consists of two summation terms that each has its own Chebyshev expansion:

$$N_e = 2\sum_{k=0}^{K^w} b_k\left(\beta^w,\mu\right) M_k^w + 2\sum_{k=0}^{K}\left[b_k\left(\beta,\mu\right) - b_k\left(\beta^w,\mu\right)\right] M_k^\Delta. \quad (13)$$

The corresponding Chebyshev moments, defined in analogy to Eq. (9), are:

$$M_k^w = \frac{1}{N_s^w}\sum_{i=1}^{N_s^w}\left\langle \chi_i^w \left| \zeta_i^{w,(k)} \right\rangle\right., \qquad M_k^\Delta = \frac{1}{N_s^\Delta}\sum_{i=1}^{N_s^\Delta}\left\langle \chi_i^\Delta \left| \zeta_i^{\Delta,(k)} \right\rangle\right. . \quad (14)$$

In practice, finding the chemical potential in both sDFT and t-sDFT involves a straightforward single-variable search. In t-sDFT, the chemical potential (Eq. (13)) is not strictly guaranteed to be monotonic with the number of electrons, since it is a summation of two terms, one of which is not necessarily positive; but in practice, we find that it is always monotonic so the determination of μ from the residues is instantaneous.

III. RESULTS

We studied three hydrogen-terminated silicon nanocrystals of different sizes, $Si_{35}H_{36}$, $Si_{87}H_{76}$, and $Si_{353}H_{196}$. Note that such nanocrystals are a convenient test ground for stochastic methods since they have small band gaps which decrease with increasing system size. As such they place a more stringent test on the method than clusters of molecules with large gaps. Metals, in contrast, require much smaller temperatures and are therefore not ideal for stochastic applications.

An LDA functional [19] was applied with norm-conserving pseudopotentials [20] using the Kleinman-Bylander form [21], and we used the Martyna-Tuckerman reciprocal-space method for treating long-range interactions [22]. The grid spacing was $0.55a_0$, and the energy cutoff was 15 Hartree for all systems. To gather sufficient statistics, $N_{\text{ind}} = 10$ independent runs with different stochastic numbers were used for each of the calculations below.

For each system, we performed calculations for several β/β^w ratios. As these systems are semiconductors, we are simply interested in the limit where the Fermi-Dirac distribution is effectively a step function. We, therefore, replace the Fermi-Dirac distribution by the complementary error function, $f_{\beta\,\mu}(\hat{h}) = \frac{1}{2}\text{erfc}(\beta(\hat{h}-\mu))$, which looks similar to the Fermi-Dirac distribution but does not require a very small β to be effectively a step function.

The numerical parameters for the runs are summarized in Table I. There are several points to note.

First, since the three systems have with increasing size a progressively smaller band gap, E_g, the larger systems require larger values of β and cor-

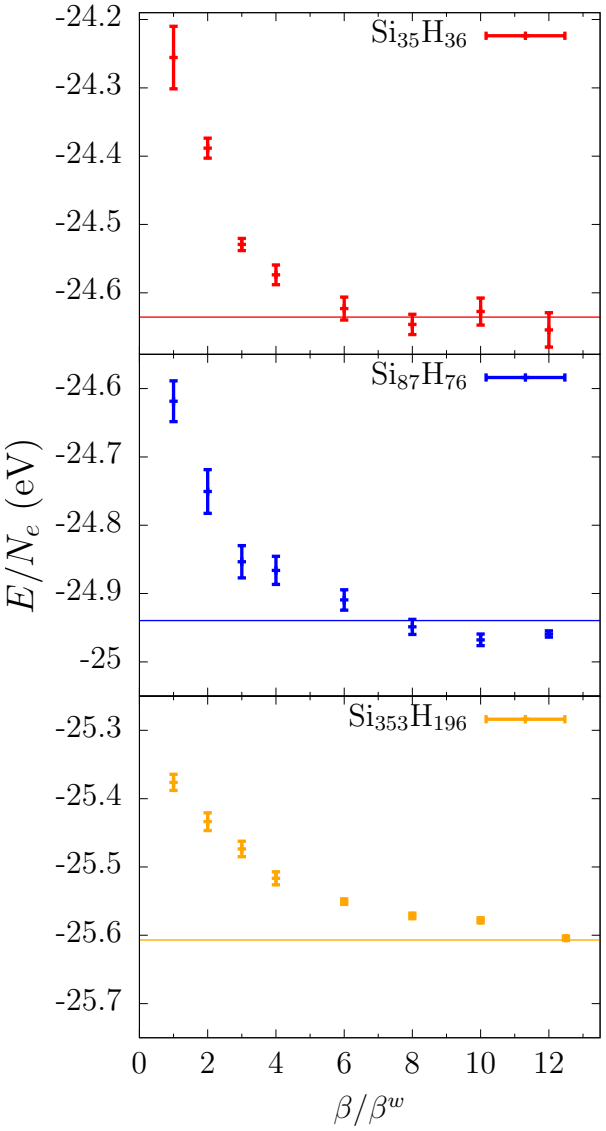

Figure 2. The energy per electron (in eV) as a function of β/β^w for three cluster sizes, based on $N_{\rm ind} = 10$ independent runs. Also included is the deterministic value in each system (horizontal line). The numerical work W, i.e., the number of Hamiltonian operations, is independent of β/β^w (see Table I for details). The leftmost point in each graph, $\beta/\beta^w = 1$, corresponds to sDFT (no tempering). Since the number of orbitals used is very small ($N_s = 30$ for sDFT), these sDFT results show marked systematic deviation (i.e., deviation of the average energy from the deterministic value) and fluctuation errors. Both types of statistical errors decrease markedly in t-sDFT, especially when $\beta/\beta^w \sim 7-10$, due to the much larger number of stochastic orbitals used in the main (warm) density part.

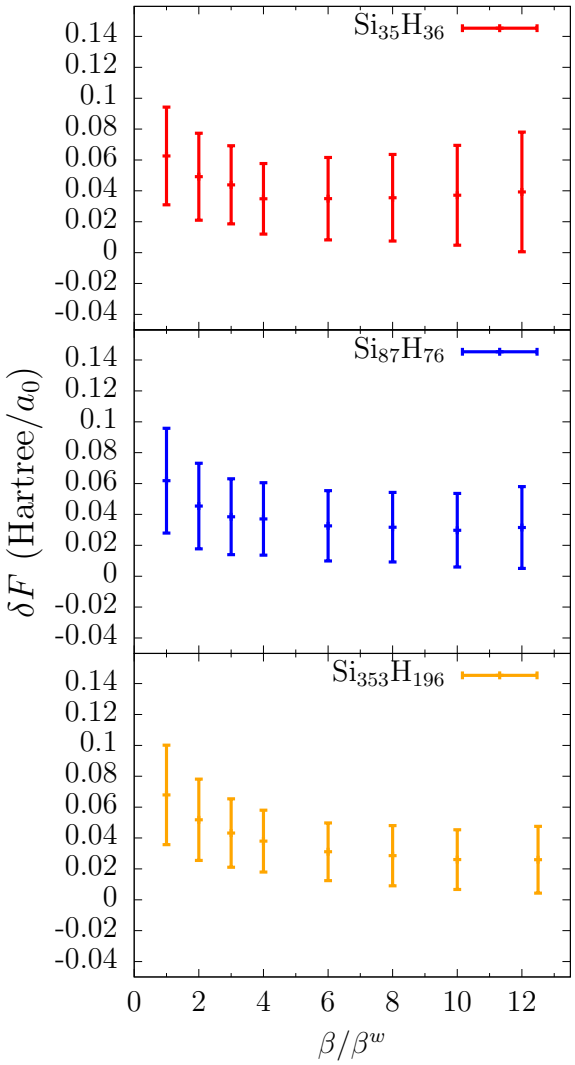

Figure 3. Analogous to Fig. 2 but shows δF,the error in the averaged force relative to the deterministic value, normalized over all silicon atoms and over the $N_{\rm ind} = 10$ runs, and the associated standard deviation σ_F (Eqs. (15,16)). In sDFT δF is significantly larger than σ_F, indicating some amount of systematic deviation. In t-sDFT, around $\beta/\beta^w \sim 7-10$, both the stochastic and especially the systematic errors decrease, i.e., σ_F decreases and $\delta F \sim \sigma_F$.

respondingly larger Chebyshev expansion lengths, K. Furthermore, we use (for all systems) $N_s = 30$ orbitals for the sDFT calculations. Finally, note that the warm temperature calculations which require most of the numerical work have an expansion length K^w and a corresponding number of stochastic orbitals N_s^w chosen so that the total work W^{tot} is the same for each value of β/β^w (this includes sDFT at $\beta/\beta^w = 1$). This allows us to compare the efficacy of

tempering in terms of the reduction of fluctuations as a function of β/β^w.

Prelude: Stochastic vs. Systematic Deviation

The results shown below exhibit two kinds of deviations, which are briefly reviewed; for a fuller discussion see Ref. [12]. The first deviation the usual stochastic Monte-Carlo fluctuation which scales with the number of samples as $N_s^{-1/2}$. The other kind is a systematic deviation. Such deviation scales as N_s^{-1} and appears whenever the results of the Monte-Carlo sampling are used in an iterative self-consistent process (see, e.g., [23]). Here, since the density is prepared from a finite number of stochastic orbitals and the filtered stochastic orbitals depend on the density, the self-consistent SCF procedure has a systematic deviation.

The practical effect of the systematic deviation is simple to state: when doing calculations with a finite N_s, and repeating these calculations many times, the averaged result would differ from the true $N_s \to \infty$ result. As we show below, in most of our calculations, tempering reduces and practically eliminates this systematic deviation, avoiding the need to use jackknife or bootstrap methods [24].

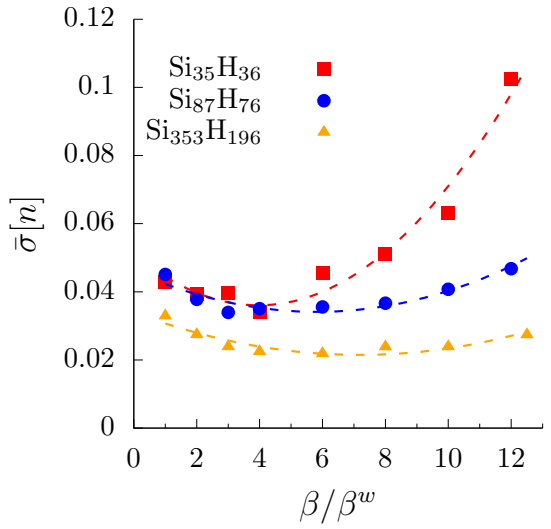

Figure 4. The normalized integral of the standard deviation of the density per electron, together with a parabolic fit. For the smaller system, the density deviation decreases between $\beta/\beta^w = 2-4$, and for the two larger systems the stochastic errors decrease around a larger range $\beta/\beta^w = 2-10$, by up to 30%-40%.

Energies

Fig. 2 shows, for the three different systems, the averaged total energies per particle based on the $N_{\rm ind} = 10$ runs and the associated error bars for different β^w values. For simplicity, the results are depicted as a function of β/β^w. In addition, we include the deterministic DFT values for comparison. Interestingly (see also the SI), for a fixed N_s, the systematic deviation decreases by a factor of 2 when the system size increases by a factor of 10, while the stochastic error decreases by a larger factor with system size, scaling as $N_e^{-1/2}$ due to self-averaging.

Consider first the starting point for each figure, $\beta/\beta^w = 1$, which is simply sDFT (i.e., with no correction terms). Since we only use $N_s = 30$ stochastic orbitals, a very small number, the sDFT calculations show a significant systematic deviation, i.e., the averaged energy-per-particle is several standard deviations away from the deterministic value.

Turning to t-sDFT (i.e., $\beta^w < \beta$), we see that both the systematic deviation and the stochastic error decrease as β/β^w increases. As evident from Fig. 2 (and verified by a second-order polynomial fit of the error in the energy as a function of β/β^w in the SI) once $\beta/\beta^w \sim 7-12$ there is essentially no systematic deviation while the stochastic fluctuations decrease by a factor of around 4-5.

The reduction in the statistical error and systematic deviation as β/β^w increases relative to sDFT ($\beta/\beta^w = 1$) for a fixed W^{tot} results from the fact that we can use a much larger number of stochastic orbitals for the warmer temperature density, the significant contribution to the density, compared to the sDFT density. Despite the need to use a longer Chebyshev expansion, we can use fewer stochastic orbitals for the correction term since its contribution to the density is smaller.

Finally note in Fig. 2, with increasing system size, the optimal β/β^w values (i.e., that results in the smallest small statistical fluctuations in the energy per electron) shift to larger ratios. This is partially a result of quantum confinement, so that with increasing size the KS gap decreases and therefore β increases, and partially due to the modified density of state structure for the larger clusters which causes the optimal β^w to increase with system size. Therefore, the smallest system the optimal ratio is about $\beta/\beta^w \sim 3-4$, and for the larger clusters minimum error is obtained for $\beta/\beta^w \sim 7-12$.

Forces and Density

We next show how t-sDFT reduces the errors in the atomic forces compared to sDFT (we only analyze the forces on the silicon atoms for comparison). Fig. 3 is similar to the energy plot in Fig. 2, but here we plot the normalized deviation of the averaged stochastic forces from the deterministic forces, δF:

$$(\delta F)^2 \equiv \frac{1}{N_{\rm Si}} \sum_{i=1}^{N_{\rm Si}} |\bar{\boldsymbol{F}}^i - \boldsymbol{F}^{d,i}|^2, \qquad (15)$$

where a bar indicates averaging over the $N_{\rm ind} = 10$ runs and "d" stands for deterministic; i is an index over the silicon atoms. The error bars in Figure 3, σ_F, indicate the standard deviation of the normalized averaged force of the silicon atoms, i.e.,

$$\sigma_F^2 = \frac{1}{(N_{\rm ind}-1)N_{\rm ind}N_{\rm Si}} \sum_{j=1}^{N_{\rm ind}} \sum_{i=1}^{N_{\rm Si}} |\boldsymbol{F}^{i,j} - \bar{\boldsymbol{F}}^i|^2, \quad (16)$$

where $\boldsymbol{F}^{i,j}$ is the force over atom i in the j'th independent run.

Note that the magnitude of the errors in the forces is large, but this could be reduced by increasing the number of independent runs or stochastic orbitals. However, since the purpose of the study is to uncover the behavior with respect to β^w, we use a small number of stochastic orbitals to reduce the computational effort and thus, apply the approach for many values of β/β^w and different system sizes. Further, note that since the stochastic errors are generally not systematic, especially once tempering is used, these forces can be used for Langevin molecular dynamics if we increase the number of sampling orbitals by about an order of magnitude. We have indeed applied sDFT (with an order of magnitude more orbitals than in this study) in a Langevin molecular dynamics study and have shown that that the Langevin dissipation matrix is then easily modified to include the effect of the fluctuations in the sDFT force, and the correct pair distribution is then obtained [25, 26].

As previously discussed, the sDFT forces are similar in the three systems, since the local environment is similar and therefore the errors are primarily a function of the number of stochastic orbitals, N_s. The reduction in the errors in the forces is appreciable but less significant than for the energy. Using again a 2nd order fit (see the SI), we get that the reduction in error in the forces is about 30% for the smallest system and goes up to 50% for the largest cluster.

To compare the deviation in the density using t-sDFT to sDFT, we use the integral of the standard deviation of the averaged density per electron, defined as $\bar{\sigma}[n] \equiv (N_{\rm ind}-1)^{-1/2} N_e^{-1} \sum \sigma(n(\boldsymbol{r}))dV$, where $\sigma(n(\boldsymbol{r}))$ is the standard deviation in the density at grid point $\boldsymbol{r}$. Fig. 4 shows that tempering again reduces the stochastic error for β/β^w values around 7-10. The reduction in the deviation of the density is similar in magnitude to that of the total atomic forces, up to 30%-40%, and is much less dramatic than the error reduction in the total energies.

Finally, note that Fig. 4 shows that when the value of β/β^w is very large, the density fluctuations start rising with the β/β^w ratio; for large ratios, the warm density deviates significantly from the low-temperature density, so the difference between the two densities is significant which causes large statistical fluctuations.

IV. CONCLUSIONS

We presented here a tempering method for stochastic density functional theory that reduces the statistical error in the total energy. Our scheme (t-sDFT) relies on decomposing the density into a large high-temperature term with a correction density. The new method expands the density in terms of the inverse temperature, β, to take advantage of the fact that with lower β (i.e., a higher effective temperature) fewer Chebyshev polynomials are needed, thus enabling the use of more stochastic orbitals without increasing the computational cost.

A natural extension of this work is the implementation of multiple-β tempering with more than two values of β, as done earlier for deterministic renormalization-group studies; the formalism is presented in Appendix A. In this work we have not implemented embedded fragments, an approach that independently reduces the standard deviation in the energy and forces. In future work, the two methods will be combined to hopefully further reduce the stochastic error. Further work will also explore how to optimize the choice of β values and the number of stochastic orbitals used to reduce the stochastic deviations.

Our method reduces the standard deviation in the total energy by a factor of around 4-5, which corresponds to reducing the total number of required stochastic orbitals by more than an order of magnitude. This is only for the total energies, while the error in the forces and density is reduced by a smaller amount only 30%-50% and 30%-40% respectively. Interestingly, this is the opposite behavior relative to energy-window sDFT where the error in the forces is improved significantly but not the error

in the total energies. Another interesting aspect is that sDFT almost eliminates systematic deviation.

The main conclusion of our work is that for the same overall cost, tempering improves the accuracy by 1.4-4 depending on the quantity studied while also shrinking the systematic deviation so that the results are closer to the deterministic value even for a small number of samples. Equivalently, for the same stochastic deviation, tempering reduces the overall effort by a factor ranging from ≈2 to ≈ 20, depending on the desired quantity.

ACKNOWLEDGMENTS

This paper was supported by the Center for Computational Study of Excited State Phenomena in Energy Materials (C2SEPEM), which is funded by the U.S. Department of Energy, Office of Science, Basic Energy Sciences, Materials Sciences and Engineering Division via Contract No. DE-AC02- 05CH11231, as part of the Computational Materials Sciences Program. In addition, RB gratefully acknowledges the support from the US-Israel Binational Science Foundation (BSF) under Grant No. 2018368. Computational resources were supplied through the XSEDE allocation TG-CHE170058.

DATA AVAILABILITY STATEMENT

The data that support the findings of this study are available from the corresponding author upon reasonable request.

APPENDIX A: MULTIPLE β

The general expansion of the filter $\hat{\rho}_\beta$ for L temperatures, ordered so $\beta \equiv \beta_1 > \beta_2 > ... > \beta_L$, is

$$\hat{\rho}_\beta = \hat{\rho}_{\beta_L} - \sum_{\ell=1}^{L-1} \Delta\hat{\rho}_\ell, \tag{17}$$

where

$$\Delta\hat{\rho}_\ell = \hat{\rho}_{\beta_{\ell+1}} - \hat{\rho}_{\beta_\ell}. \tag{18}$$

This expansion leads to an expression for the density similar to Eqs. 11-12. The case we studied in the paper is simply $L = 2$, with $\beta_1 \equiv \beta$ and $\beta_2 \equiv \beta^w$.

[1] R. O. Jones. Density functional theory: Its origins, rise to prominence, and future. *Reviews of Modern Physics*, 87(3):897–923, August 2015.

[2] Brian Kolb and T Thonhauser. Molecular Biology at the Quantum Level: Can Modern Density Functional Theory Forge the Path? *Nano LIFE*, 2(02), 2012.

[3] Daniele Selli, Gianluca Fazio, and Cristiana Di Valentin. Modelling realistic TiO_2 nanospheres: A benchmark study of SCC-DFTB against hybrid DFT. *The Journal of Chemical Physics*, 147(16):164701, 2017. Publisher: AIP Publishing LLC.

[4] Christoph Freysoldt, Blazej Grabowski, Tilmann Hickel, Jörg Neugebauer, Georg Kresse, Anderson Janotti, and Chris G. Van de Walle. First-principles calculations for point defects in solids. *Rev. Mod. Phys.*, 86(1):253–305, March 2014. Publisher: American Physical Society.

[5] Roi Baer and Martin Head-Gordon. Sparsity of the Density Matrix in Kohn-Sham Density Functional Theory and an Assessment of Linear System-Size Scaling Methods. *Phys. Rev. Lett.*, 79(20):3962–3965, November 1997.

[6] G. E. Scuseria. Linear scaling density functional calculations with Gaussian orbitals. *J. Phys. Chem. A*, 103(25):4782–4790, 1999.

[7] T. Ozaki. Efficient low-order scaling method for large-scale electronic structure calculations with localized basis functions. *Phys. Rev. B*, 82(7):075131, 2010.

[8] Carlos Romero-Muniz, Ayako Nakata, Pablo Pou, David R Bowler, Tsuyoshi Miyazaki, and Rubén Pérez. High-accuracy large-scale DFT calculations using localized orbitals in complex electronic systems: The case of graphene–metal interfaces. *Journal of Physics: Condensed Matter*, 30(50):505901, 2018. Publisher: IOP Publishing.

[9] Roi Baer, Daniel Neuhauser, and Eran Rabani. Self-Averaging Stochastic Kohn-Sham Density-Functional Theory. *Phys. Rev. Lett.*, 111(10):106402, September 2013.

[10] Daniel Neuhauser, Roi Baer, and Eran Rabani. Communication: Embedded fragment stochastic density functional theory. *J. Chem. Phys.*, 141(4):041102, 2014.

[11] Ming Chen, Roi Baer, Daniel Neuhauser, and Eran Rabani. Overlapped embedded fragment stochastic density functional theory for covalently-bonded materials. *J. Chem. Phys.*, 150(3):034106, January 2019.

[12] Marcel D. Fabian, Ben Shpiro, Eran Rabani, Daniel Neuhauser, and Roi Baer. Stochastic density functional theory. *Wiley Interdisciplinary Reviews: Computational Molecular Science*,

10.1002/wcms.1412(0):e1412, 2019.

[13] Ming Chen, Roi Baer, Daniel Neuhauser, and Eran Rabani. Energy window stochastic density functional theory. *J. Chem. Phys.*, 151(11):114116, September 2019.

[14] Ming Chen, Roi Baer, Daniel Neuhauser, and Eran Rabani. Stochastic density functional theory: Real- and energy-space fragmentation for noise reduction. *J. Chem. Phys.*, 154(20):204108, May 2021.

[15] Roi Baer and Martin Head-Gordon. Energy renormalization-group method for electronic structure of large systems. *Physical Review B-Condensed Matter*, 58(23):15296–15299, 1998.

[16] Michael F Hutchinson. A stochastic estimator of the trace of the influence matrix for Laplacian smoothing splines. *Commun Stat Simul Comput.*, 19(2):433–450, 1990.

[17] R. Kosloff. Time-Dependent Quantum-Mechanical Methods for Molecular- Dynamics. *J. Phys. Chem.*, 92(8):2087–2100, 1988.

[18] Otto F Sankey, David A Drabold, and Andrew Gibson. Projected random vectors and the recursion method in the electronic-structure problem. *Phys. Rev. B*, 50(3):1376, 1994.

[19] J.P. Perdew and Y. Wang. Accurate and Simple Analytic Representation of the Electron-Gas Correlation-Energy. *Phys. Rev. B*, 45(23):13244–13249, 1992.

[20] N. Troullier and J. L. Martins. Efficient Pseudopotentials for Plane-Wave Calculations. *Phys. Rev. B*, 43(3):1993–2006, 1991.

[21] Leonard Kleinman and D. M. Bylander. Efficacious Form for Model Pseudopotentials. *Phys. Rev. Lett.*, 48(20):1425–1428, May 1982.

[22] G. J. Martyna and M. E. Tuckerman. A reciprocal space based method for treating long range interactions in ab initio and force-field-based calculations in clusters. *J. Chem. Phys.*, 110(6):2810–2821, 1999.

[23] Daniel Neuhauser, Roi Baer, and Dominika Zgid. Stochastic self-consistent second-order Green's function method for correlation energies of large electronic systems. *J. Chem. Theory Comput.*, 13:5396–5403, 2017.

[24] Jun Shao and C. F. J. Wu. A general theory for jackknife variance estimation. *The Annals of Statistics*, 17(3):1176–1197, 1989.

[25] Eitam Arnon, Eran Rabani, Daniel Neuhauser, and Roi Baer. Equilibrium configurations of large nanostructures using the embedded saturated-fragments stochastic density functional theory. *J. Chem. Phys.*, 146(22):224111, June 2017.

[26] Eitam Arnon, Eran Rabani, Daniel Neuhauser, and Roi Baer. Efficient Langevin dynamics for "noisy" forces. *The Journal of Chemical Physics*, 152(16):161103, April 2020.